Received: 16 December 2019 | Revised: 19 June 2020 | Accepted: 22 June 2020

DOI: 10.1111/liv.14594

ORIGINAL ARTICLE

Liver INTERNATIONAL WILEY

Interaction between CHOP and FoxO6 promotes hepatic lipid accumulation

Dae Hyun Kim[1] | Byeong Moo Kim[1] | Ki Wung Chung[1,2] | Yeon Ja Choi[3] | Byung Pal Yu[4] | Hae Young Chung[1]

[1]Department of Pharmacy, College of Pharmacy, Pusan National University, Geumjeong-Gu, Busan, Korea

[2]Department of Pharmacy, College of Pharmacy, Kyungsung University, Nam-gu, Busan, Korea

[3]Department of Biopharmaceutical Engineering, Division of Chemistry and Biotechnology, College of Science and Technology, Dongguk University, Gyeongju, Korea

[4]Department of Physiology, The University of Texas Health Science Center at San Antonio, TX, USA

Correspondence
Hae Young Chung, College of Pharmacy, Pusan National University, 2, Busandaehak-ro 63beon-gi, Geumjeong-Gu, Busan 46241, Korea.
Email: hyjung@pusan.ac.kr

Funding information
the National Research Foundation of Korea (NRF) grant funded by the Korea government, Grant/Award Number: 2018R1A2A3075425

Handling Editor: Utpal Pajvani

Abstract

Background & Aims: Endoplasmic reticulum (ER) stress is one of the major causes of hepatic insulin resistance through increasing de novo lipogenesis. Forkhead box O6 (FoxO6) is a transcription factor mediating insulin signalling to glucose and lipid metabolism, therefore, dysregulated FoxO6 is involved in hepatic insulin resistance. In this study, we elucidated the role of FoxO6 in ER stress-induced hepatic lipogenesis.

Methods: Hepatic ER stress responses and lipogenesis were monitored in mice overexpressed with constitutively active FoxO6 allele and FoxO6-null mice. In the in vitro study, HepG2 cells overexpressing constitutively active FoxO6 were treated with palmitate, and then alterations in ER stress and lipid metabolism were measured.

Results: FoxO6 activation induced hepatic lipogenesis and the expression of ER stress-inducible genes. The expression and transcriptional activity of peroxisome proliferator-activated receptor γ (PPARγ) were significantly increased in constitutively active FoxO6 allele. Interestingly, we found that the active FoxO6 physically interacted with C/EBP homologous protein (CHOP), an ER stress-inducible transcription factor, which was responsible for PPARγ expression. Palmitate treatment caused the expression of ER stress-inducible genes, which was deteriorated by FoxO6 activation in HepG2 cells. Palmitate-induced ER stress led to PPARγ expression through interactions between CHOP and FoxO6 corresponding to findings in the in vivo study. On the other hand, the expression of PPARα and β-oxidation were decreased in constitutively active FoxO6 allele which implied that lipid catabolism is also regulated by FoxO6.

Conclusion: Our data present significant evidence demonstrating that CHOP and FoxO6 interact to induce hepatic lipid accumulation through PPARγ expression during ER stress.

KEYWORDS

CHOP, ER stress, FoxO6, lipogenesis, PPARγ

1 | INTRODUCTION

Forkhead box O (FoxO) transcription factors induce target genes involved in the regulation of cellular metabolic pathways. The FoxO subfamily of proteins, including FoxO1, FoxO3, FoxO4 and FoxO6, are characterized by a highly conserved, winged-helix DNA-binding motif. Furthermore, FoxO proteins act as Akt substrates to mediate the inhibitory effect of insulin (or IGF-1) on key genes involved in cell survival, proliferation, differentiation, oxidative stress and metabolism in mammals.[1] For instance, the phosphorylation of FoxO by Akt, in response to insulin or other growth factors, allows FoxO to be translocated from the nucleus to the cytoplasm.[1-3] Suppressed growth factor signalling activates FoxO because of the Akt-induced FoxO inhibition, whereas elevated certain fatty acids, such as palmitate, activate FoxO via a distinct mechanism involving the c-Jun N-terminal kinase (JNK) pathway.[4] Endoplasmic reticulum (ER) stress has been associated with the JNK pathway through IRE1-mediated activation of JNK signalling.[5,6] JNK phosphorylates the insulin receptor substrate (IRS) proteins and limits the activation of phosphatidylinositol-3-kinase (PI3K)/Akt signalling in response to insulin.

The function of FoxO6 in hepatic lipid metabolism and its possible contribution to hypertriglyceridemia in type 2 diabetes remain unclear. Although increased ER stress results in insulin resistance, the molecular mechanism by which ER stress causes aberrant insulin responses has not been completely elucidated. Martinez *et al*[7] investigated the nutrient-regulated cellular localization and activity of FoxO1 in β-cells and found that the gene encoding the nutrient-regulated C/EBP homologous protein (CHOP) was a potential transcriptional target of FoxO1. However, both CHOP and FoxO3 may regulate apoptosis.[8] Here we report a similar mechanism for ER stress that acts via the protein kinase IRE-1 and PERK, which overrides the insulin-mediated inhibition of FoxO6 activity. ER stress has been suggested to be a crucial common factor in hepatic lipogenesis, liver-specific inflammation and insulin resistance.[9,10]

ER stress also induces serine phosphorylation of IRS-1 via the JNK pathway, inhibits insulin response in cultured liver cells,[6,11] enhances lipogenesis, affects hepatic steatosis and influences insulin resistance.[12] However, these inferences were drawn from studies conducted in genetically obese or prolonged chronic high-fat feeding models,[6,13] which have not provided reasonable insights into the effect of ER stress on de novo lipogenesis or lipid influx. The unfolded protein response (UPR) is induced by the accumulation of unfolded protein aggregates or excessive protein trafficking.[14,15] Arsenic can activate the UPR, which is initiated by IRE-1, PERK and ATF6.[16] ATF4, ATF6 and XBP1 regulate the transcription of several genes such as CHOP10, which is one of the genes highly expressed during ER stress.[15] However, C/EBPβ initially induces the expression of peroxisome proliferator-activated receptor γ (PPARγ) and C/EBPα, which then form a positive feedback loop by activating each other's expression and eventually contribute to the induction and maintenance of expression of adipocyte-specific genes.[17,18] To investigate the potential relationship between FoxO6 and other ER stress-related molecules in HepG2 cells, CHOP expression was examined. CHOP plays a critical role in apoptosis induced by ER stress.[19]

In the present study, we investigated the role of FoxO6 in upregulating PPARγ expression through ER stress-induced CHOP activation in the liver and HepG2 cells to achieve a better understanding of the molecular mechanisms involved in hepatic lipogenesis.

2 | MATERIALS AND METHODS

2.1 | Materials

All chemical reagents were obtained from Sigma (St. Louis, MO, USA), except where noted. Western blotting detection reagents were obtained from Amersham (Bucks, UK). RNAzol™ B was obtained from TEL-TEST Inc (Friendwood, TX, USA). Antibodies against α-tubulin (sc-5286), β-actin (sc-47778), TFIIB (sc-271736), Histone H1 (sc-8615), p-Akt (sc-101629), total-Akt (sc-1618), p-PERK (sc-32577), PERK (sc-13073), IRE (sc-390960), ATF6 (sc-22799), CHOP (sc-575), PPARγ (sc-7196), pS-IRS (sc-33956), pT-IRS (sc-17196), IRS (sc-559) and SREBP-1c (sc-365513) were obtained from Santa Cruz Biotechnology (Santa Cruz, CA, USA). Antibodies against p-IRE (ab48187), PPARα (ab24509), CPT1α (ab128568) and Acox1 (ab184032) were purchased from Abcam (Cambridge, UK). Antibodies against FoxO6 and p-FoxO6 (Ser184) were obtained from Dr Dong (University of Pittsburgh, Pittsburgh, PA, USA). Horseradish peroxidase-conjugated anti-rabbit IgG and horseradish peroxidase-conjugated anti-mouse IgG antibodies were obtained from Amersham (Bucks, UK). Horseradish peroxidase-conjugated anti-sheep/goat IgG from donkey was purchased from Serotec (Oxford, UK). Polyvinylidene difluoride (PVDF) membranes were obtained from Millipore Corporation (Bedford, MA, USA). PPARα-siRNA (20 nmol/L) was obtained from Integrated DNA Technologies (IDT; Coralville, Iowa).

2.2 | Animal experimental procedures

C57BL/6J male mice aged 6 weeks were purchased from the Jackson Laboratory. The mice received standard rodent chow and water ad libitum and were kept in sterile cages with a 12 hours light/dark cycle. The C57BL/6J mice were weighed and randomly assigned to two groups; the mice in one group received an intravenous tail injection of an adenoviral vector containing a constitutively active FoxO6 allele (AdV-FoxO6-CA), whereas the mice in the other group received an intravenous tail injection of an AdV-null vector, both at 1.5×10^{11} plaque forming units (pfu)/kg body weight. The mice were sacrificed 2 weeks after the AdV-FoxO6-CA injection. The mice had fasted for 24 h, and venous blood samples were collected from the tail in order to determine blood glucose levels as previously described.

The FoxO6-knockout (FoxO6-KO) male mice aged 8 weeks were fed standard rodent chow or a high fat diet (fat content, 60 kcal%; Research Diets, Inc, New Brunswick, NJ), depending on the group they were in, and were provided water ad libitum. The mice were

kept in sterile cages, with a 12 h light/dark cycle. The livers from FoxO6-KO mice were obtained from the University of Pittsburgh Medical Center (Dr Dong, University of Pittsburgh, PA, USA).

The animal protocols used in this study were reviewed and approved for ethical procedures and scientific care by the Institutional Animal Care and Use Committee at Pusan National University (PNU-IACUC).

2.3 | Cell culture

HepG2 cells were purchased from American Type Culture Collection (ATCC, Virginia, USA). Cells were cultured in Dulbecco's modified Eagle's medium (DMEM, Lonza, Walkersville, MD) and were transduced with an Adv-FoxO6-CA vector expressing the constitutively active FoxO6 allele as previously described.[20] The Adv-Empty vector was used as a control. The Adv-FoxO6-siRNA vector expressing the FoxO6-specific siRNA and Adv-Sc-siRNA vector encoding scrambled siRNA have been previously described.[20] The Adv-Akt-CA vector encodes a constitutively active form of Akt, as previously described.[21] All adenoviral vectors were produced in HEK293 cells, as previously described.[22]

2.4 | Transfection and luciferase assay

For a peroxisome proliferator response element (PPRE; 5′-GATCCCCGAACGTGACCTTTGTCCTGGTCC-3′)-driven luciferase assay, 1×10^4 HepG2 cells were seeded per well into a 48-well cell culture plate. The PPRE-X3-TK-LUC plasmid (0.5 μg) (a kind gift from Dr Christoper K. Glass, University of California, San Diego, CA, USA) and 0.5 μg of full-length human PPARγ expression vectors (kind gifts from Dr Han Geuk Seo, Konkuk University, Seoul, South Korea) were transfected into the cells using 0.5 μg DNA/0.5 μL Lipofectamine 2000 (Invitrogen, Carlsbad, CA, USA) complexes in 500 μL normal media containing 10% serum, incubated for 24 hours and then treated with the scrambled or CHOP-siRNA (40 nmol/L). After incubation for 4 hours, the transfection medium was replaced with fresh medium, and cells were incubated for an additional 48 hours. Subsequently, 500 μM of palmitate was added, and after 8 h incubation, the cells were washed with phosphate-buffered saline (PBS). Luciferase activity was analysed by the Steady-Glo Luciferase Assay System (Promega, Madison, WI, USA), and was measured using a luminometer (GENious, TECAN, Salzburg, Austria).

2.5 | Biochemical analysis

Blood samples were collected from each group of mice. Different kits were used according to the manufacturer's instructions to determine the concentrations of the following metabolites in the serum: insulin (Shibayagi, Japan), glucose, non-esterified fatty acids (NEFA) and TG (Shinyang, South Korea).

2.6 | Glucose tolerance test

Mice were fasted for 24 hours, followed by an intraperitoneal injection of glucose (2 g/kg). Blood glucose levels were measured before and after the glucose injection using a Glucometer Elite meter (Bayer, IN, USA).

2.7 | Western blot analysis

Homogenized samples were boiled for 5 minutes with a gel-loading buffer (0.125 M Tris-HCl, pH 6.8, 4% sodium dodecyl sulphate (SDS), 10% 2-mercaptoethanol and 0.2% bromophenol blue) at a 1:1 ratio. Equal amounts of total protein from each sample were separated by SDS-polyacrylamide gel electrophoresis (SDS-PAGE) using 10% acrylamide gels and transferred to PVDF membranes at 80 V for 1.5 hours in a semidry transfer system. The membranes were immediately placed in blocking buffer (5% non-fat milk in 10 mmol/L Tris at pH 7.5, 100 mmol/L NaCl and 0.1% Tween 20). The blot was blocked at room temperature for 30 minutes. The membrane was incubated with a specific primary antibody at 4°C overnight, followed by a horse radish peroxidase-conjugated anti-rabbit antibody at room temperature for 1.5 hours. Labelled antibodies were detected using Westsave™ (Abfromtier, South Korea). Prestained protein markers were used for molecular weight determinations.

2.8 | Hepatic lipid content

Liver tissues or cells (20 mg) were homogenized in 400 μL of HPLC-grade acetone. After an overnight incubation with agitation at room temperature, 50 μL aliquots of acetone-extracted lipid suspensions were used to determine triglyceride concentrations via the Infinity triglyceride reagent (Thermo Electron). Hepatic lipid content was defined as milligrams of triglyceride per gram of total liver proteins, as described earlier.

2.9 | RNA isolation and real-time quantitative reverse transcriptase PCR (qRT-PCR)

RNA was isolated from liver tissue or cells using the RNeasy Mini Kit (QIAGEN, Valencia, CA). qRT-PCR analysis was performed to quantify mRNA concentrations using the SYBR Green and the CFX Connect System (Bio-Rad Laboratories Inc, Hercules, CA, USA). The primers used are shown in Table S1. All primers were purchased from IDT (Coralville, IA).

2.10 | Chromatin immunoprecipitation (ChIP) assay

ChIP was used to study the interaction between FoxO6 and the PPARγ promoter DNA in cells. HepG2 cells (2×10^5 cells) were transfected with

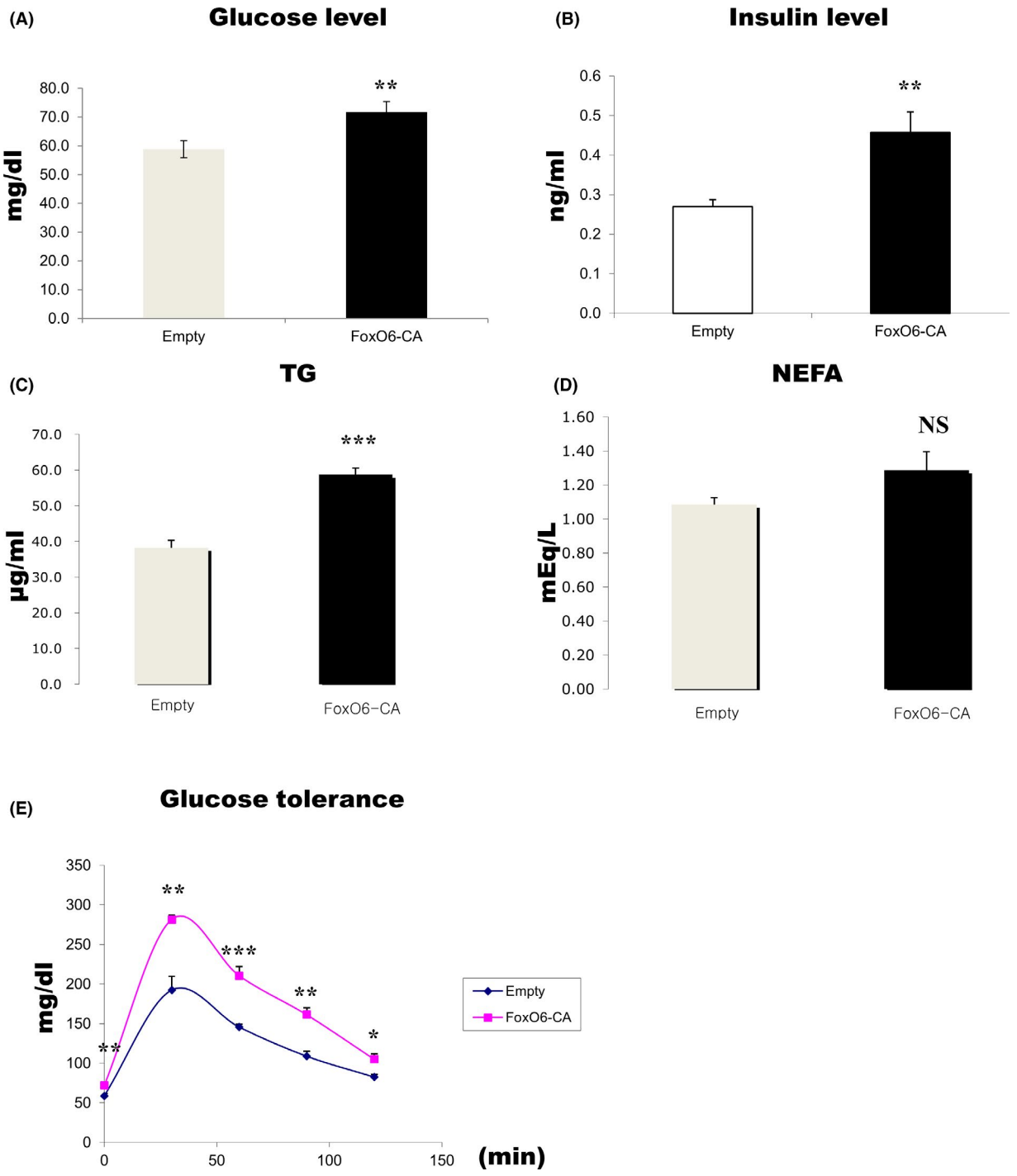

FIGURE 1 Effects of FoxO6 on insulin resistance and hyperlipidemia. Levels of serum in empty vector and FoxO6-CA virus-injected mice measured for 14 days (n = 5). (A) Fasting blood glucose levels. (B) Fasting plasma insulin levels. (C) Triglyceride levels, (D) free fatty acid and (E) glucose tolerance test. Mice were fasted for 16 h, followed by determination of fasting blood glucose levels. Results of one-way ANOVA: $^{**}P < .01$, $^{***}P < .001$ vs empty vector

pGH11 in triplicate, in the presence of a FoxO6 vector at a multiplicity of infection (MOI) of 100 pfu/cell. After 24 hours incubation, cells were subjected to a ChIP assay using the anti-FoxO6 antibody and the ChIP assay kit (Upstate Biotechnology). The immunoprecipitates were analysed by immunoblot analysis using a rabbit anti-FoxO6 antibody, and by PCR to detect co-immunoprecipitated DNA, using PPARγ promoter-specific primers (forward 5′-CATTCGCCTTCATAACATTC-3′, reverse 5′-CTTGCTCCTCACAGCCGCT-3′) that flank the consensus FoxO6 binding-site in the human PPARγ promoter (Dr Dong, University of Pittsburgh, PA, USA).

2.11 | Immunoprecipitation (IP) of tissue extracts

Liver tissue extracts were immunoprecipitated in a buffer containing 40 mmol/L Tris-HCl (pH 7.6), 120 mmol/L NaCl, 20 mmol/L glycerophosphate, 20 mmol/L NaF, 2 mmol/L sodium orthovanadate, 5 mmol/L ethylenediaminetetraacetic acid (EDTA), 1 mmol/L phenylmethylsulfonyl fluoride (PMSF), 0.1% NP40 containing leupeptin (2 μg/mL), aprotinin (1 μg/mL), and pepstatin A (1 μg/mL). Aliquots of cell extracts were centrifuged at 12,000*g* at 4°C for 15 min, incubated overnight at 4°C with the required antibody, and then incubated overnight at 4°C in a 50% protein A agarose slurry. After washing the immunoprecipitates three times with IP buffer, immunoprecipitated proteins were analysed by SDS-PAGE, and western blotting analysis was performed as described above.

2.12 | Histological analysis

The Oil red O staining was performed as previously described with optimal cutting temperature of frozen tissues to visualize lipid accumulation.

2.13 | Immunostaining

HepG2 cells were seeded at 1×10^4 cells per well in a six-well plate, incubated for 24 h, fixed in 4% paraformaldehyde solution (15 min at room temperature), washed with PBS buffer, blocked with 3% normal goat serum (Gibco, Grand Island, USA) and immunostained using a rabbit anti-FoxO6 antibody (1:500 dilution) at 4°C overnight. Cells were then washed with TBS and incubated for 3 h in the presence of anti-rabbit IgG labelled with Alexa Fluor 488 (1:200; Invitrogen, CA, USA). Cell nuclei were visualized by immunostaining with Hoechst 33 342 (1:1000; Invitrogen), and FoxO6 localization was determined by confocal laser scanning microscopy (TCS SP2, Leica, Wetzler, Germany).

2.14 | Statistical analyses

All data are expressed as mean ± SEM. Treatments were compared by one-way ANOVA followed by Dunnett's post hoc test. p-values < 0.05 were considered statistically significant.

3 | RESULTS

3.1 | FoxO6 induces hyperinsulinemia and hyperlipidemia

Obesity generally accompanies alterations in glucose tolerance and the blood lipid profile, which are closely associated with hepatic steatosis. To examine whether FoxO6-induced lipid accumulation occurs in the liver, we measured triglyceride content in liver homogenates.

Male mice developed hyperinsulinemia and hypertriglyceridemia after injection with a constitutively active FoxO6-CA allele, and consequently showed high levels of fasting glucose, insulin and plasma TG levels (Figure 1A–C). Plasma NEFA levels showed no change (Figure 1D). However, glucose tolerance was impaired in FoxO6-CA mice compared with empty virus-injected mice (Figure 1E).

3.2 | FoxO6 upregulates lipid accumulation

To determine whether FoxO6 plays a role in relating lipogenesis gene expression to aberrant ER stress, and characterize the underlying mechanism, we determined the hepatic expression of genes involved in lipogenesis and fatty acid oxidation, two opposing pathways in hepatic lipid metabolism, in FoxO6 virus-injected (FoxO6-CA) liver. FoxO6-CA resulted in significant reduction of β-oxidation, as reflected by significantly decreased nuclear level of PPARα (Figure 2A). FoxO6-CA mice exhibited significantly increased protein levels of the nuclear PPARγ (Figure 2A), the activation of which is linked to enhanced lipid synthesis and increased fat storage in the liver. However, level of the nuclear ER stress gene CHOP was increased in FoxO6-CA mice (Figure 2A). FoxO6-CA resulted in significant induction in lipogenesis, as reflected by significantly increased levels of fatty acid synthase (FAS), sterol regulatory element-binding protein (SREBP-1), acetyl-coenzyme A carboxylase (ACC) and PPARγ mRNAs in the liver of FoxO6-CA mice. This effect was accompanied by decreased expression of carnitine palmitoyltransferase (CPT) and acyl-coenzyme A oxidase 1(ACOX1) (Figure 2B), two key enzymes involved in fatty acid oxidation through PPARα. We measured hepatic TG content, and found that FoxO6-CA mice were associated with increased fat content in the liver compared to control littermates (Figure 2C), consistent with the notion that FoxO6 promotes hepatic lipogenesis. These results were confirmed by Oil red O staining of FoxO6-CA livers (Figure 2D). FoxO6 is a transcription factor that is negatively regulated by Akt during insulin signalling. FoxO6 dephosphorylation enhances its stability and activity, thereby stimulating gluconeogenesis and hyperlipidemia. PPARγ expression was suppressed by various concentrations of Akt vector (Figure S1A). In addition, immunoprecipitation results showed that the interaction between FoxO6 and PPARγ was induced in Akt overexpressed cells (Figure S1B). We analysed FoxO6-stimulated PPARγ activation in HepG2 cells. FoxO6 was found to bind PPARγ promoter, as determined by a chromatin immunoprecipitation assay (Figure S2). Furthermore, FoxO6 increased transcriptional activity of PPARγ using PPRE/PPARγ luciferase assay with the empty vector and FoxO6-CA-transduced HepG2 cells (Figure S2B). However, in the immunoprecipitation study, an interaction between FoxO6 and CHOP was demonstrated in the liver. As shown in Figure 2E, the interaction between CHOP and FoxO6 was increased in FoxO6-CA livers. We examined insulin signalling in the livers of FoxO6-CA-injected mice. As shown in Figure 2F, treatment with FoxO6-CA suppressed insulin signalling.

3.3 | Effect of FoxO6 on palmitate-induced ER stress in HepG2 cells

The transcriptional activities of FoxO family proteins have been previously demonstrated to increase when insulin levels were

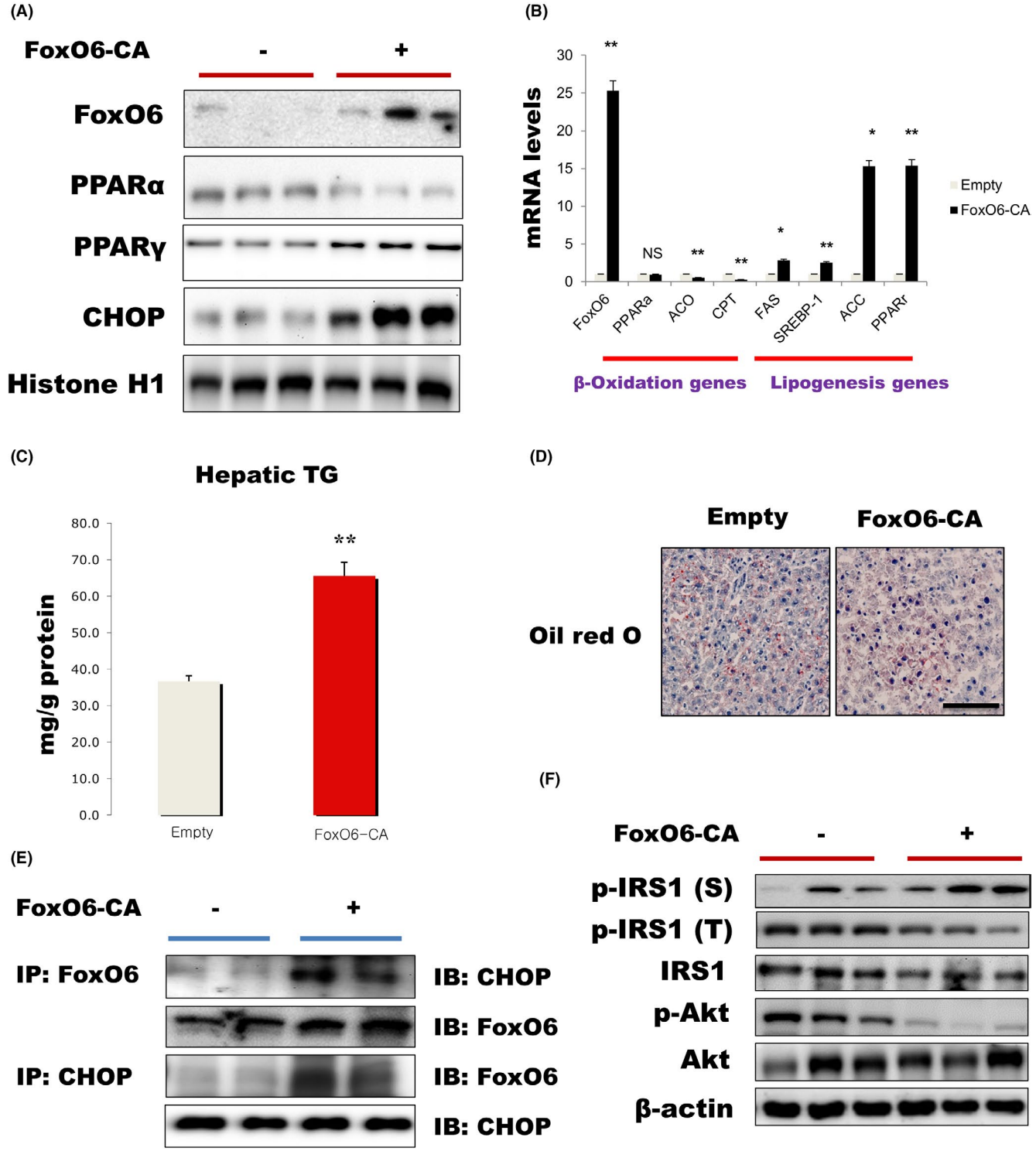

FIGURE 2 FoxO6 regulates lipid accumulation in FoxO6-CA-injected liver. (A) Western blot analysis was used to detect FoxO6, PPARα, PPARγ and CHOP in the nuclear extracts (20 μg protein) from liver tissues. (B) β-oxidation and lipogenesis genes were subjected to real-time qRT-PCR analysis. Results of one-way ANOVA: $^{*}P < .05$, $^{**}P < .01$ vs empty vector. (C) Triglyceride levels in hepatic tissues. Results of one-way ANOVA: $^{**}P < .01$ vs empty vector. (D) Livers were stained with Oil red O to visualize lipid accumulation. (E) Western blot analysis showed that immunoprecipitated FoxO6 and CHOP were physically associated with CHOP and FoxO6 respectively. (F) Insulin signalling factors (pSer-IRS1, pTyr-IRS1, IRS1, p-Akt and Akt level). β-actin acts as the loading control for the cytosolic fractions

reduced.[2] We examined the expression of ER stress genes in FoxO6-CA-transduced HepG2 cells. Treatment of cells with ER stress activators (brefeldin, tunicamycin and thapsigargin) decreased FoxO6 phosphorylation (Figure S3). These data collectively indicate that ER stress induces FoxO6 activation. To examine the hypothesis that FoxO6 targets and transactivates ER stress genes, we conducted

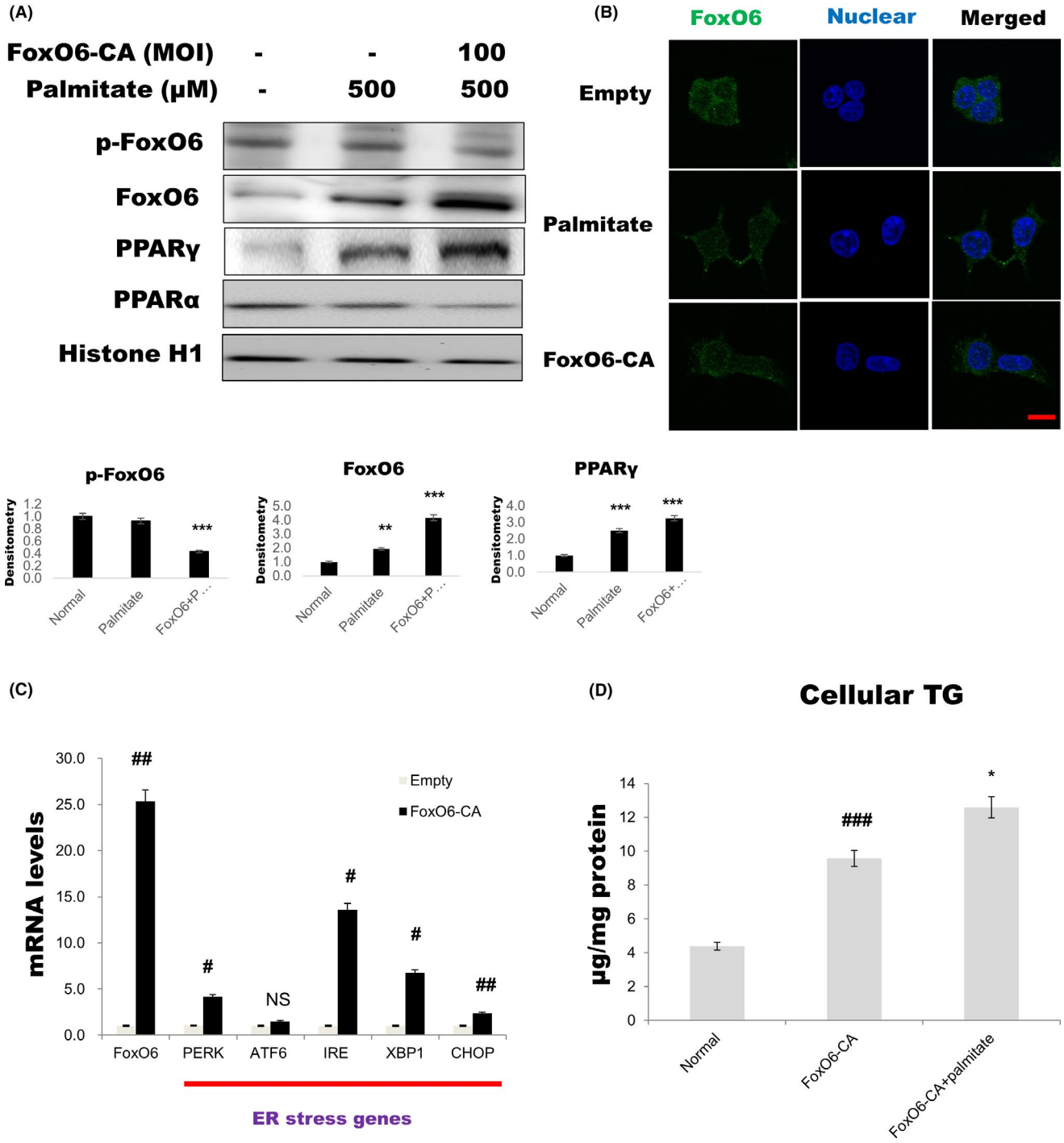

FIGURE 3 Lipid accumulation by palmitate-induced ER stress in liver cells. HepG2 cells were transfected with FoxO6-CA vector at 100 MOI. After incubation for 24 h, cells were treated with palmitate. (A) Western blot analysis was used to detect p-FoxO6, total-FoxO6, PPARα and PPARγ in nuclear extracts from liver cells. Histone H1 acts as the loading control for the nuclear fractions. Results are representative of three independent experiments. Bars in densitometry data represent means ± SE, and significance was determined using an unpaired t test: $^{**}P < .01$, $^{***}P < .001$ vs Normal. (B) HepG2 cells were treated with palmitate (500 μmol/L) or FoxO6 vector for 24 h. Cells were immunostained using rabbit an anti-FoxO6 antibody followed by IgG conjugated with fluorescein isothiocyanate (green). Bar = 50 μm. (C) Real-time PCR analyses was performed for measuring the mRNA levels of FoxO6, PERK, ATF6, IRE, XBP1 and CHOP. Results of one factor ANOVA: $^{\#}P < .05$, $^{\#\#}P < .01$ vs empty vector virus. (D) Triglyceride levels in cells. Results of one-way ANOVA: $^{\#\#\#}P < .001$ vs empty vector; $^{*}P < .05$ vs FoxO6-CA

studies to assess the palmitate-induced expression of ER stress genes in HepG2 cells. As a result, palmitate enhanced p-IRE, p-PERK and CHOP levels (Figure S4). Lipid accumulation associated with FoxO6 was determined by western blot assays and qRT-PCR analyses with palmitate and FoxO6-CA-transduced HepG2 cells. These results indicated that treatment with FoxO6-CA or palmitate

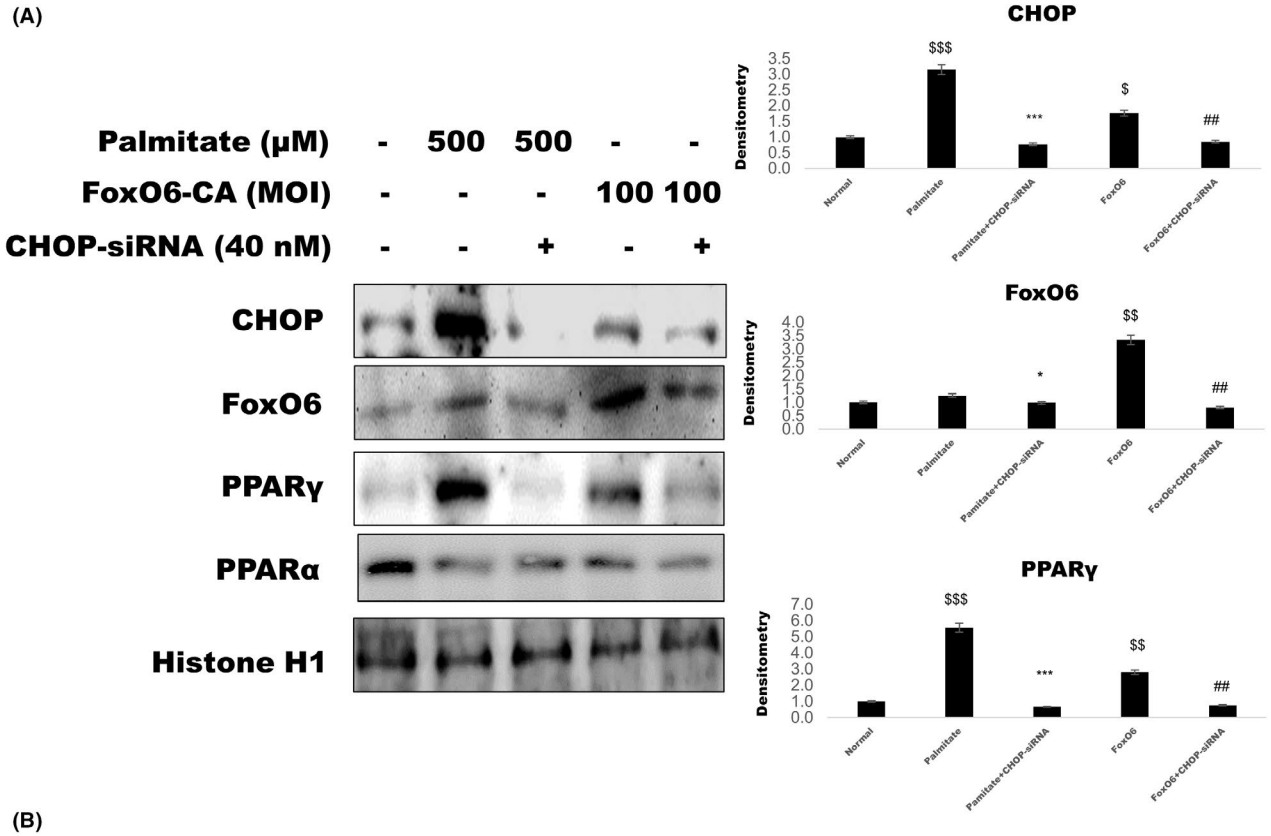

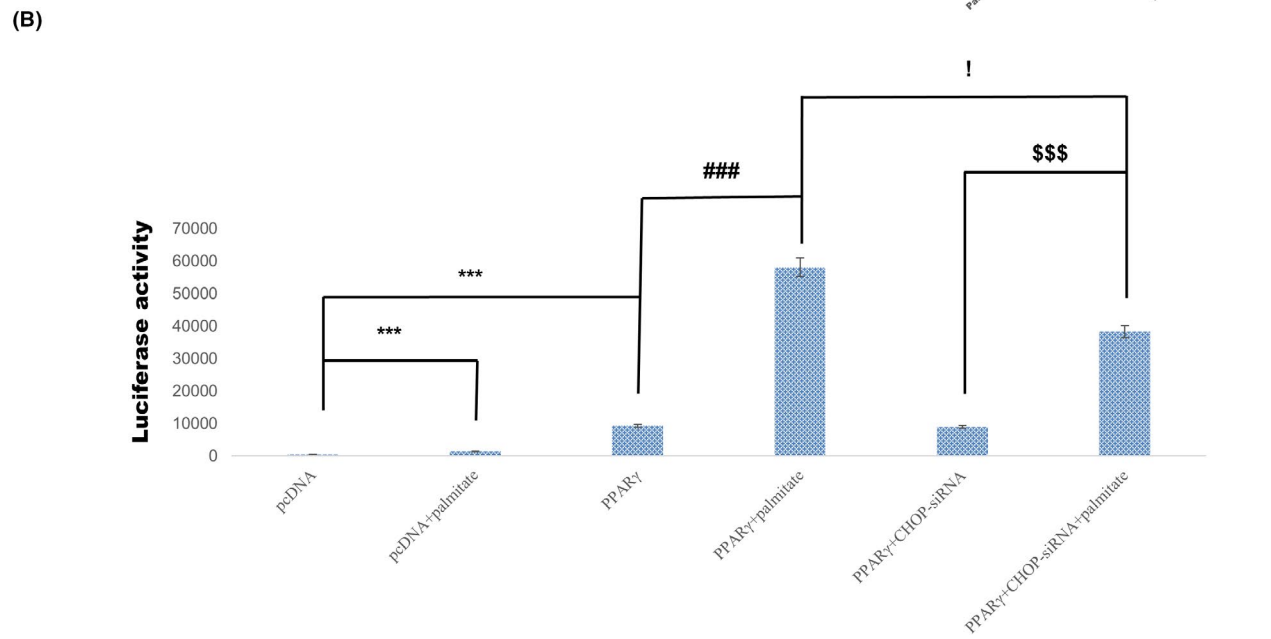

FIGURE 4 Induction of PPARγ expression and activation by FoxO6 through CHOP. (A) HepG2 cells were grown to 80% confluence in 100 mm dishes in DMEM, pretreated (1 day) with or without CHOP-siRNA (40 nmol/L), stimulated with FoxO6-CA (100 MOI) and anasyzed by western blotting. Histone H1 acts as the loading control for the nuclear fractions. Results are representative of three independent experiments. Bars in densitometry data represent means ± SE, and significance was determined using an unpaired t test: $^{\$}P < .05$, $^{\$\$}P < .01$, $^{\$\$\$}P < .001$ vs Normal; $^{*}P < .05$, $^{***}P < .001$ vs Palmitate; $^{\#\#}P < .01$ vs FoxO6-CA. (B) Effect of palmitate, with or without CHOP-siRNA (40 nmol/L), on PPARγ activity. HepG2 cells in 48-well microplates were transduced with CHOP-siRNA (40 nmol/L) or control Adv-null vectors, followed by transfection with 0.5 μg pcDNA, full-length human PPARγ and peroxisome proliferator responsive element (PPRE) promoter luciferase DNA in culture medium. After 24 h incubation, cells were treated with palmitate (500 μmol/L) for 8 h and then harvested to determine luciferase activities. The relative luciferase promoter activity was calculated from the ratio of luciferase activity. $^{***}P < .001$ vs pcDNA; $^{\#\#\#}P < .001$ vs PPARγ; $^{\$\$\$}P < .001$ vs PPARγ+CHOP-siRNA; $^{!}P < .05$ vs PPARγ + palmitate

had an enhanced stimulatory effect on the level of FoxO6 and PPARγ (Figure 3A). However, combining FoxO6-CA with palmitate treatment further decreased PPARα level (Figure 3A). This effect was accompanied by increased expression of PERK, IRE, XBP1 and CHOP mRNAs (Figure 3C). These observations support the idea that FoxO6 regulates transactivation of PPARγ, and thus contributes to the regulation of palmitate. As shown in Figure 3B, palmitate treatment induced a remarkable shift of FoxO6 from the cytoplasm to the nucleus as determined by immunostaining. However, FoxO6 increased cellular TG levels in combination with palmitate compared to cells treated with FoxO6-CA alone (Figure 3D). These results indicated that FoxO6 or palmitate have enhanced stimulatory effects on lipid accumulation.

3.4 | Effect of CHOP loss-of-function on PPARγ level and activity by palmitate-mediated FoxO6 in HepG2 cells

In order to determine the roles of CHOP and FoxO6, HepG2 cells were treated with CHOP-siRNA, FoxO6-CA and palmitate. As a result, palmitate enhanced FoxO6, CHOP and PPARγ expression (Figure 4). In addition, palmitate treatment decreased nuclear PPARα level. These results indicated that treatment with palmitate had an enhanced stimulatory effect on the level of CHOP, FoxO6 and PPARγ. However, treatment with CHOP-siRNA and palmitate suppressed FoxO6 and PPARγ levels compared with palmitate treatment alone. CHOP-siRNA treatment also reduced PPARγ and FoxO6 levels (Figure 4A). To examine palmitate-induced PPARγ activity in HepG2 cells, the PPRE/PPARγ-luciferase assay was performed and revealed that palmitate was associated with increased activity of PPARγ. However, in the absence of CHOP, PPARγ activity induced by palmitate was decreased (Figure 4B). Palmitate-mediated FoxO6 was found to be associated with increased PPARγ activity in CHOP-siRNA-transduced cells, compared to the empty vector in HepG2 cells.

3.5 | Changes in the expression of ER stress genes in FoxO6-KO liver

To characterize the role of FoxO6 in glucose metabolism, Calabuig-Navarro *et al*[23] bred FoxO6$^{+/-}$ heterozygous mice to generate homozygous KO mice (FoxO6-KO) that were viable. To determine the effect of lipid accumulation on FoxO6 depletion, we analysed lipogenesis gene levels. Significant differences were observed in the expression levels of β-oxidation and lipogenesis genes between FoxO6-KO and WT littermates on a high fat diet. We also measured ER stress levels, and observed significant differences in the expression of ER stress genes in the liver of FoxO6-KO mice (vs WT littermates) via western blotting (Figure 5A), as well as qPCR (Figure 5B). We also measured levels of lipogenesis genes by western blotting and qPCR. These results showed a significant decrease in FoxO6, CHOP and PPARγ protein levels in FoxO6-KO mice vs WT littermates (Figure 5A). However, FoxO6-KO increased PPARα level in liver tissues (Figure 5A). Furthermore, compared with control littermates, FoxO6-KO mice showed increased expression of β-oxidation-associated genes. The mRNA levels of lipogenesis genes such as PPARγ, FASN and SCD1 were also decreased in the FoxO6-KO liver (Figure 5B). Collectively, these data underscore the importance of the β-oxidation pathway in FoxO6-induced lipogenesis in liver cells, especially under excessive ER stress.

3.6 | PPARα deficiency increases liver lipid accumulation

To confirm the role of PPARα in FoxO6-CA-induced lipid accumulation, we subjected liver cells to PPARα-siRNA and FoxO6-CA, and first compared changes in lipid metabolism. As expected, FoxO6-CA showed decreased PPARα and β-oxidation-associated gene expression (Figure 6, A and B). Compared with FoxO6-CA, PPARα-siRNA led to reduced expression of β-oxidation-associated proteins and genes (Figure 6, A and B). In contrast, other lipid metabolism genes, such as lipogenesis genes, were not changed with PPARα-siRNA treatment (Figure 6B). FoxO6-CA combined with PPARα-siRNA led to significantly higher lipid accumulation compared with FoxO6-CA alone (Figure 6C). These data indicate that PPARα deficiency significantly decreases β-oxidation with high lipid accumulation in liver cells.

4 | DISCUSSION

Our study characterized FoxO6 as a novel transcription factor that independently mediates hepatic lipogenesis during ER stress. We demonstrated crosstalk between FoxO6, CHOP, and ER stress-induced hepatic lipogenesis. The lipotoxicity of non-alcoholic fatty liver disease (NAFLD) is caused by lipid oversupply that directly influences the balance between ER homoeostasis and ER stress.[24]

Thus far, little was known about FoxO6 (a member of the FoxO family) and its regulatory role in ER stress-induced lipogenesis. Our data suggests that ER stress induces FoxO6 activation (Figure S3). Consequently, constitutive FoxO6 expression is observed in cells transfected with inactivated CHOP, as shown by ER stress-induced CHOP-mediated regulation of FoxO6 expression (Figure 4). When ER homoeostasis was disturbed, unfolded proteins accumulate in the ER lumen, which consequently activates the UPR through dissociation of immunoglobulin protein/78 kDa glucose-regulated protein (BiP/GRP78) from PERK, IRE1α and ATF6α.[25,26] Paradoxically, under these conditions, translation of ATF4 mRNA was selectively enhanced, which induced transcription of CHOP.[27] ER stress induction increased the CHOP response to a greater extent than the induction of DNA damage.[15] Miyazaki *et al*[28] investigated the regulatory role of CHOP in myocardial reperfusion injury in a CHOP-KO mouse model. They found that the ER stress-induced CHOP pathway was involved in myocardial ischemia/reperfusion injury leading to cardiomyocyte

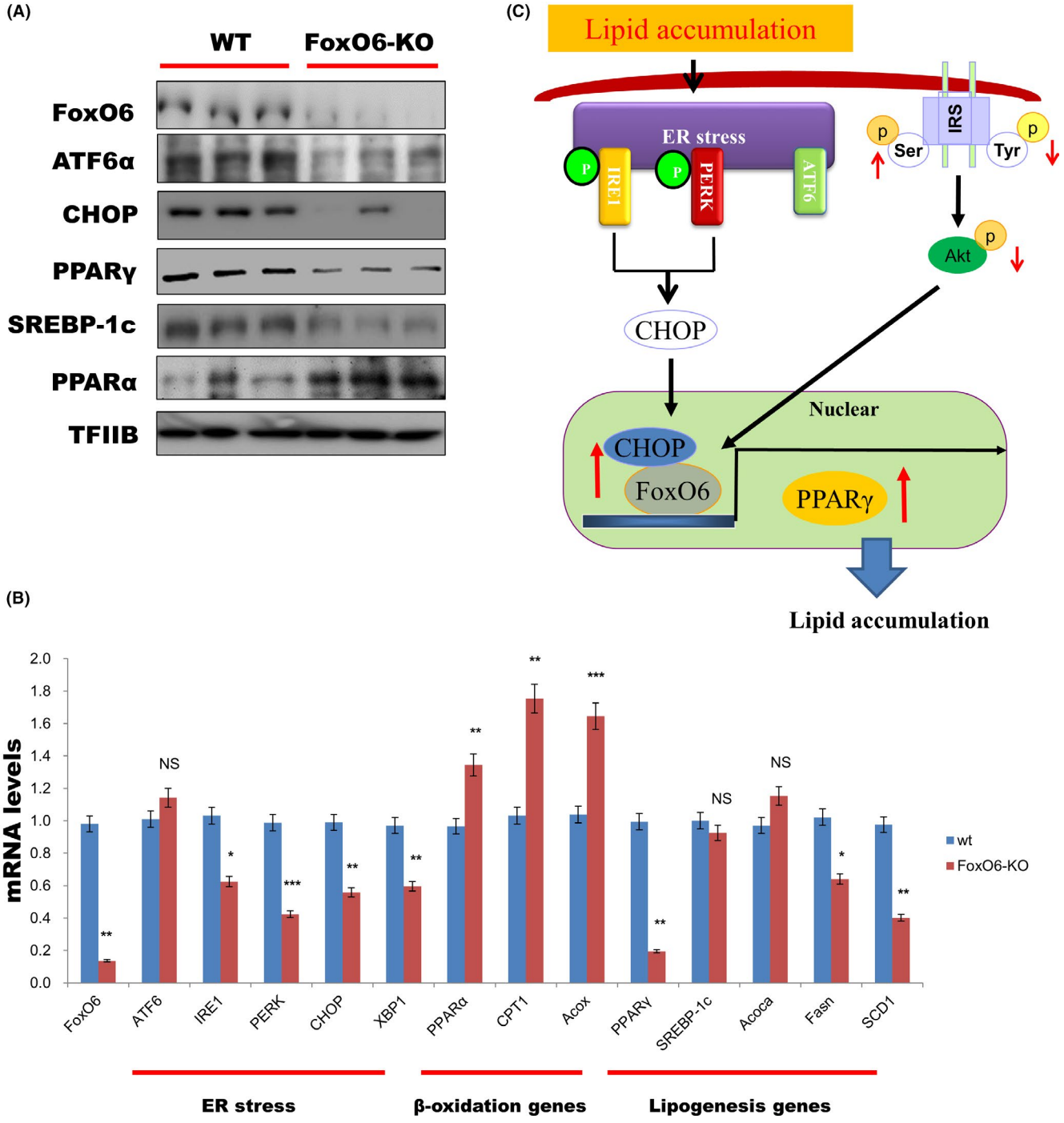

FIGURE 5 Effect of FoxO6 depletion on lipid metabolism and ER stress in FoxO6-KO mice. Mice were fed a high fat diet at 4 weeks of age for 12 weeks (n = 6). (A) Nuclear proteins were subjected to semiquantitative immunoblot analysis for FoxO6, ATF6, CHOP, PPARγ, SREBP-1c and PPARα, and TFIIB was used as a loading control for the nuclear fractions. (B) Expression levels of FoxO6, ER stress genes (ATF6, IRE1, PERK, CHOP and XBP1), β-oxidation genes (PPARα, CPT1 and Acox) and lipogenesis genes (PPARγ, SREBP-1c, Acoca, Fasn and SCD1) were analysed by qPCR. Results were normalized to β-actin mRNA levels. $^{*}P < .05$, $^{**}P < .01$ and $^{***}P < .001$ vs wild-type control. NS, not significant. (C) Possible mechanism for how FoxO6 activates ER stress in lipogenesis

apoptosis and myocardial inflammation. Additionally, CHOP may physically interact with FoxO3, a common upstream regulator of Puma and Bim transcription in neuronal cells during ER stress.[8] Furthermore, nuclear translocation of FoxO1 triggered apoptosis and CHOP translocation from the cytoplasm to nucleus under ER-stress.[29]

This effect, which helped suppress TG overproduction and attenuate steatosis in the insulin-resistant liver, contributed to the increase in free fatty acid and glucose levels in plasma in FoxO6-CA-injected mice (Figure 1). In addition, FoxO6 was associated with elevated lipogenesis, contributing to increased fat accumulation in the liver of FoxO6-CA-injected mice (Figure 1). To investigate

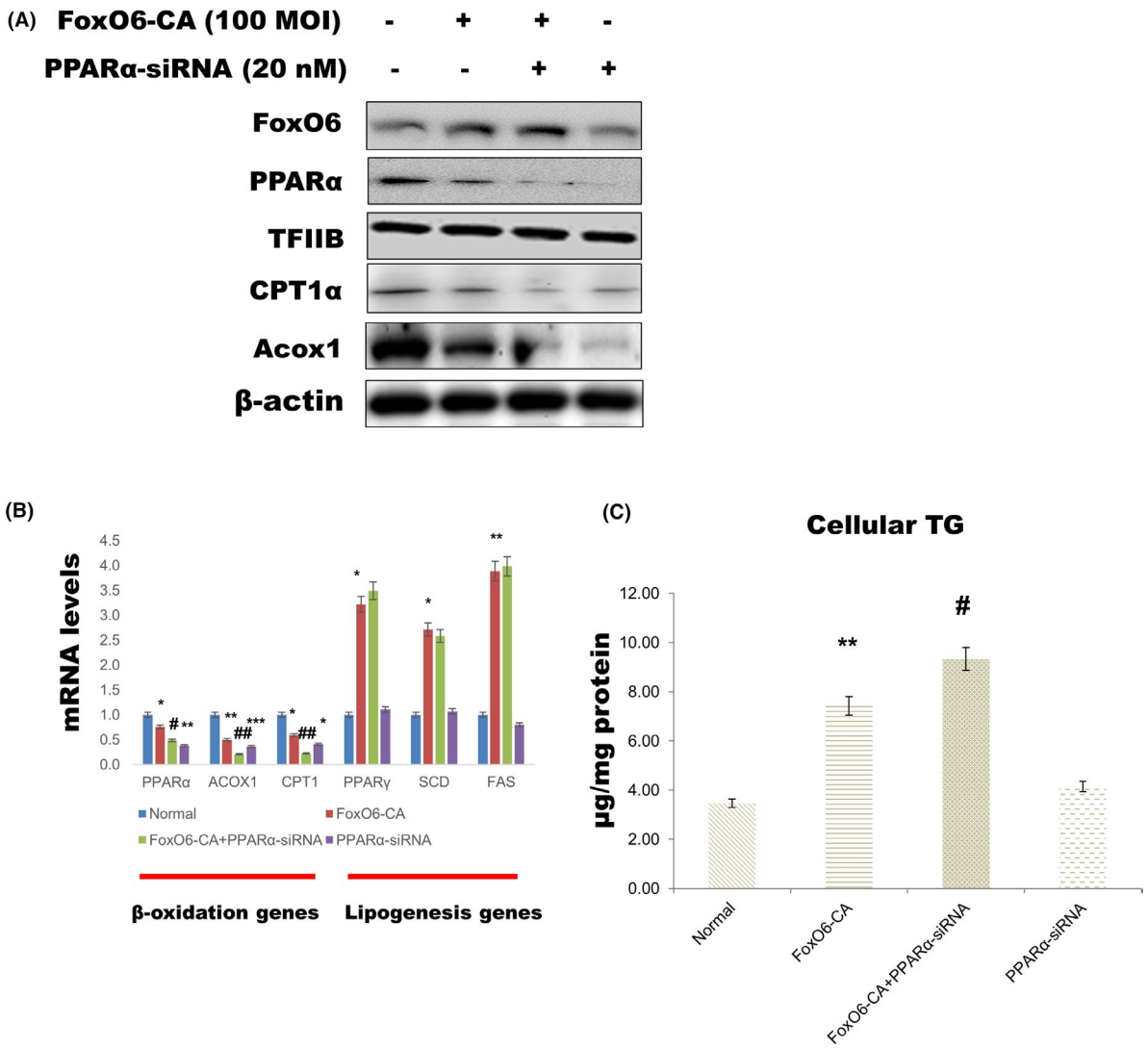

FIGURE 6 PPARα deficiency increases liver lipid accumulation. PPARα-siRNA was subjected to FoxO6-CA to investigate the effect of PPARα on liver lipid metabolism during FoxO6-CA treatment. (A) HepG2 cells were grown to 80% confluence in 100 mm dishes in DMEM, pretreated (1 day) with or without PPARα-siRNA (20 nmol/L), stimulated (1 day) with FoxO6-CA (100 MOI) and analysed by western blotting. Nuclear protein expression of FoxO6, PPARα and cytosolic protein expression of CPT1α and ACOX1 were measured by western blotting. TFIIB and β-actin were used as the respective loading controls. (B) Gene expression levels of β-oxidation and lipogenesis targets were measured by qPCR. $^{*}P < .05$, $^{**}P < .01$, $^{***}P < .001$ vs normal. $^{\#}P < .05$, $^{\#\#}P < .01$ vs FoxO6-CA. (C) HepG2 cells were treated with PPARα-siRNA (20 nmol/L) or FoxO6-CA vector for 48 h. TGs were quantified in the liver cells. $^{**}P < .01$ vs normal. $^{\#}P < .05$ vs FoxO6-CA

the underlying mechanism, we showed that hepatic expression of PPARγ, SREBP-1c, FAS and ACC genes was significantly upregulated, and the level of IRS/Akt protein decreased in the liver of FoxO6-CA-injected mice (Figure 2). Fatty liver is a common secondary disease in obesity,[30] type 2 diabetes and possibly insulin resistance. The strong association between hepatic steatosis and insulin resistance in human[31] and animal models[32,33] suggests that insulin resistance may cause pathogenesis in obesity-related fatty liver disease. An increase in lipotoxicity has been known to lead to insulin signalling. In this study, we present evidence that ER stress can affect hepatic fat accumulation via FoxO6 activity.

FoxO6 was shown to trigger hepatic expression of the PPARγ transcription factor. These data further underscore the critical role of PPARγ in promoting hepatic lipogenesis and storage in insulin resistance. In support of this notion, we showed that hepatic PPARγ level significantly decreased in response to FoxO6 knockdown in the insulin resistant liver, resulting in the suppression of hepatic lipogenesis (Figure 5). This effect was likely derived from FoxO6-mediated inhibition of fatty acid oxidation. PPARγ is a nuclear receptor that complexes with the retinoid X receptor to promote lipogenesis in the liver. In the liver, specific PPARγ depletion attenuates lipogenesis and diminishes hepatic fat infiltration, protecting against fat-induced steatosis in mice. It has been widely established that PPARγ stimulates hepatic lipid accumulation.[34-37] Close association between increased PPARγ expression and hepatic steatosis was demonstrated by increasing lipogenic gene expression in genetically engineered and diet-induced obese mice.[34,35,37] Although numerous studies have reported that both FoxO6 and PPARγ

stimulate hepatic steatosis, the molecular relationship between PPARγ and FoxO6 in the liver remained unclear. Our data showed that FoxO6 directly binds to the PPARγ promoter region, and this binding was strongly increased during hepatic steatosis, possibly due the significant increase in PPARγ expression after FoxO6-CA treatment. However, FoxO6-CA significantly increased liver lipid accumulation and decreased the expression of PPARα and β-oxidation-associated genes (Figure 6). These data also suggest that the FoxO6-mediated increase in PPARγ activity at least partially contributed to the increase in hepatic lipid accumulation.

In summary, lipid accumulation during ER stress and suppressed IRS/Akt signalling induces FoxO6 activation, which consequently results in hepatic lipogenesis gene expressions. Under ER stress, FoxO6 interacted with CHOP, upregulated PPARγ and inhibited PPARα in the mouse liver and HepG2 cells (Figure 5C). These results provide significant insights into the molecular and cellular basis of the association between FoxO6 and CHOP, suggesting these as novel molecular targets for potential hepatic lipogenesis therapeutics.

ACKNOWLEDGEMENTS

This work was supported by a National Research Foundation of Korea (NRF) grant funded by the Korean government (MSIT) (2018R1A2A3075425). In addition, this research was supported by the Basic Science Research Program through the National Research Foundation of Korea (NRF) funded by the Ministry of Education (NRF-2018R1A6A3A11046180). The authors are grateful to the Aging Tissue Bank (Busan, Korea) for supplying the research materials used in this work. We thank Dr H. Henry Dong (Children's Hospital of Pittsburgh of UPMC, Pittsburgh, PA) for providing assistance in generating FoxO6-KO mice.

CONFLICT OF INTEREST

The authors declare no conflict of interest.

AUTHOR CONTRIBUTIONS

DHK, KWC, YJC and BMK collected the samples and performed the experiments. DHK, BPY and HYC wrote the manuscript. All authors contributed to the interpretation of the results. All authors revised and approved the manuscript.

ORCID

Hae Young Chung https://orcid.org/0000-0002-3215-8828

REFERENCES

1. Accili D, Arden KC. FoxOs at the crossroads of cellular metabolism, differentiation, and transformation. *Cell*. 2004;117:421-426.
2. Barthel A, Schmoll D, Unterman TG. FoxO proteins in insulin action and metabolism. *Trends endocrinol Metabo*. 2005;16:183-189.
3. Biggs WH, Meisenhelder J, Hunter T, Cavenee WK, Arden KC. Protein kinase B/Akt mediated phosphorylation promotes nuclear exclusion of the winged helix transcription factor FKHR1. *Proc Natl Acad Sci USA*. 1999;96:7421-7426.
4. Kawamori D, Kaneto H, Nakatani Y, et al, The forkhead transcription factor Foxo1 bridges the JNK pathway and the transcription factor PDX-1 through its intracellular translocation. *J Biol Chem*. 2006;281:1091-1098.
5. Urano F, Bertolotti A, Ron D. IRE1 and efferent signaling from the endoplasmic reticulum. *J Cell Sci*. 2000;113:3697-3702.
6. Ozcan U, Cao Q, Yilmaz E, et al, Hotamisligil, Endoplasmic reticulum stress links obesity, insulin action, and type 2 diabetes. *Science*. 2004;306:457-461.
7. Martinez SC, Cras-Meneur C, Bernal-Mizrachi E, Permutt MA. Glucose regulates Foxo1 through insulin receptor signaling in the pancreatic islet beta-cell. *Diabetes*. 2006;55:1581-1591.
8. Ghosh AP, Klocke BJ, Ballestas ME, Roth KA. CHOP potentially co-operates with FOXO3a in neuronal cells to regulate PUMA and BIM expression in response to ER stress. *PLoS One*. 2012;7:e39586.
9. Ozcan U, Yilmaz E, Ozcan L, et al. Chemical chaperones reduce ER stress and restore glucose homeostasis in a mouse model of type 2 diabetes. *Science*. 2006;313:1137-1140.
10. Lee AH, Glimcher LH. Intersection of the unfolded protein response and hepatic lipid metabolism. *Cell Mol Life Sci*. 2009;66:2835-2850.
11. Hotamisligil GS. Endoplasmic reticulum stress and the inflammatory basis of metabolic disease. *Cell*. 2010;140:900-917.
12. Lee AH, Scapa EF, Cohen DE, Glimcher LH. Regulation of hepatic lipogenesis by the transcription factor XBP1. *Science*. 2008;320:1492-1496.
13. Savage DB, Choi CS, Samuel VT, et al, Reversal of diet-induced hepatic steatosis and hepatic insulin resistance by antisense oligonucleotide inhibitors of acetyl-CoA carboxylases 1 and 2. *J Clin Invest*. 2006;116:817-824.
14. Banhegyi G, Baumeister P, Benedetti A, et al, Endoplasmic reticulum stress. *Ann NY Acad Sci*. 2007;1113:58-71.
15. Oyadomari S, Mori M. Roles of CHOP/GADD153 in endoplasmic reticulum stress. *Cell Death Differ*. 2004;11:381-389.
16. Oh RS, Pan W-C, Yalcin A, et al, Functional RNA interference (RNAi) screen identifies system A neutral amino acid transporter 2 (SNAT2) as a mediator of arsenic-induced endoplasmic reticulum stress. *J Biol Chem*. 2012;287:6025-6034.
17. Rosen ED, MacDougald OA. Adipocyte differentiation from the inside out. *Nat Rev Mol Cell Biol*. 2006;7:885-896.
18. Tontonoz P, Spiegelman BM. Fat and beyond: the diverse biology of PPARγ. *Annu Rev Biochem*. 2008;77:289-312.
19. Kim R, Emi M, Tanabe K, Murakami S. Role of the unfolded protein response in cell death. *Apoptosis*. 2006;11:5-13.
20. Kim DH, Perdomo G, Zhang T, et al, FoxO6 integrates insulin signaling with gluconeogenesis in the liver. *Diabetes*. 2011;60:2763-2774.
21. Kamagate A, Qu S, Perdomo G, et al, FoxO1 mediates insulin-dependent regulation of hepatic VLDL production in mice. *J Clin Invest*. 2008;118:2347-2364.
22. Altomonte J, Cong L, Harbaran S, et al, Foxo1 mediates insulin action on ApoC-III and triglyceride metabolism. *J Clin Invest*. 2004;114:1493-1503.
23. Calabuig-Navarro V, Yamauchi J, Lee S, et al, Forkhead Box O6 (FoxO6) depletion attenuates hepatic gluconeogenesis and protects against fat-induced glucose disorder in mice. *J Biol Chem*. 2015;290:15581-15594.
24. Leamy AK, Egnatchik RA, Young JD. Molecular mechanisms and the role of saturated fatty acids in the progression of non-alcoholic fatty liver disease. *Prog Lipid Res*. 2013;52:165-174.
25. Walter P, Ron D. The unfolded protein response: from stress pathway to homeostatic regulation. *Science*. 2011;334:1081-1086.
26. Wang S, Kaufman RJ. The impact of the unfolded protein response on human disease. *J Cell Biol*. 2012;197:857-867.

27. Harding HP, Zhang Y, Zeng H, et al, An integrated stress response regulates amino acid metabolism and resistance to oxidative stress. *Mol Cell*. 2003;11:619-633.
28. Miyazaki Y, Kaikita K, Endo M, et al, C/EBP homologous protein deficiency attenuates myocardial reperfusion injury by inhibiting myocardial apoptosis and inflammation. *Arterioscler Thromb Vasc Biol*. 2011;31:1124-1132.
29. Ye Z, Wang N, Xia P, Wang E, Liao J, Guo Q. Parecoxib suppresses CHOP and Foxo1 nuclear translocation, but increases GRP78 levels in a rat model of focal ischemia. *Neurochem Res*. 2013;38:686-693.
30. Silverman JF, Pories WJ, Caro JF. Liver pathology in diabetes mellitus and morbid obesity. *Pathol Annu*. 1989;24:275-302.
31. Marceau P, Biron S, Hould F-S, et al, Liver pathology and the metabolic syndrome X in severe obesity. *J Clin Endocrinol Metab*. 1999;84:1513-1517.
32. Uysal KT, Wiesbrock SM, Marino MW, Hotamisligil GS. Protection from obesity-induced insulin resistance in mice lacking TNF-alpha function. *Nature*. 1997;389:610-614.
33. Shimomura I, Bashmakov Y, Horton JD. Increased levels of nuclear SREBP-1c associated with fatty livers in two mouse models of diabetes mellitus. *J Biol Chem*. 1999;274:30028-30032.
34. Ables GP. Update on PPARγ and nonalcoholic fatty liver disease. *PPAR Res*. 2012;2012:912351.
35. Inoue M, Ohtake T, Motomura W, et al, Increased expression of PPARgamma in high fat diet-induced liver steatosis in mice. *Biochem Biophys Res Commun*. 2005;336:215-222.
36. Matsusue K, Haluzik M, Lambert G, et al, Liver-specific disruption of PPARgamma in leptin-deficient mice improves fatty liver but aggravates diabetic phenotypes. *J Clin Invest*. 2003;111:737-747.
37. Yu S, Matsusue K, Kashireddy P, et al, Adipocyte-specific gene expression and adipogenic steatosis in the mouse liver due to peroxisome proliferator-activated receptor gamma1 (PPARgamma1) overexpression. *J Biol Chem*. 2003;278:498-505.

SUPPORTING INFORMATION

Additional supporting information may be found online in the Supporting Information section.

How to cite this article: Kim DH, Kim BM, Chung KW, Choi YJ, Yu BP, Chung HY. Interaction between CHOP and FoxO6 promotes hepatic lipid accumulation. *Liver Int*. 2020;40:2706–2718. https://doi.org/10.1111/liv.14594